Protein Expression and Purification 164 (2019) 105464

Contents lists available at ScienceDirect

Protein Expression and Purification

journal homepage: www.elsevier.com/locate/yprep

Heterologous expression, purification and biochemical characterization of a new endo-1,4-β-xylanase from *Rhodothermaceae* bacterium RA

Kok Jun Liew[a], Chen Yi Ngooi[a], Mohd Shahir Shamsir[a], Rajesh Kumar Sani[b], Chun Shiong Chong[a], Kian Mau Goh[a,*]

[a] Faculty of Science, Universiti Teknologi Malaysia, 81310, Skudai, Johor, Malaysia
[b] Department of Chemical and Biological Engineering, South Dakota School of Mines and Technology, Rapid City, USA

ARTICLE INFO

Keywords:
GH10
Glycosyl hydrolase
Rhodothermaceae
Xylanase

ABSTRACT

Xylanases (EC 3.2.1.8) are essential enzymes due to their applications in various industries such as textile, animal feed, paper and pulp, and biofuel industries. Halo-thermophilic *Rhodothermaceae* bacterium RA was previously isolated from a hot spring in Malaysia. Genomic analysis revealed that this bacterium is likely to be a new genus of the family *Rhodothermaceae*. In this study, a xylanase gene (1140 bp) that encoded 379 amino acids from the bacterium was cloned and expressed in *Escherichia coli* BL21(DE3). Based on InterProScan, this enzyme XynRA1 contained a GH10 domain and a signal peptide sequence. XynRA1 shared low similarity with the currently known xylanases (the closest is 57.2–65.4% to *Gemmatimonadetes* spp.). The purified XynRA1 achieved maximum activity at pH 8 and 60 °C. The protein molecular weight was 43.1 kDa XynRA1 exhibited an activity half-life ($t_{1/2}$) of 1 h at 60 °C and remained stable at 50 °C throughout the experiment. However, it was NaCl intolerant, and various types of salt reduced the activity. This enzyme effectively hydrolyzed xylan (beechwood, oat spelt, and *Palmaria palmata*) and xylodextrin (xylotriose, xylotetraose, xylopentaose, and xylohexaose) to produce predominantly xylobiose. This xylanase is the first functionally characterized enzyme from the bacterium, and this work broadens the knowledge of GH10 xylanases.

1. Introduction

Xylan, a typical hemicellulose composition, constitutes about one-third of the total dry weight in plants [1]. Complete degradation of xylan is achieved by the synergy actions of different enzymes, including xylanase (EC 3.2.1.8), beta-xylosidase (EC 3.2.1.37), alpha-L-arabinofuranosidase (EC 3.2.1.55), acetyl xylan esterase (EC 3.1.1.72), ferulic/coumaric acid esterase (EC 3.1.1.73), alpha-glucuronidase (EC 3.2.1.139), and other enzymes. Among the list mentioned above, xylanase (synonym: endo-1,4-β-xylanase) is one of the crucial biocatalysts to hydrolyze the β-1,4-glycosidic bonds of the xylan backbone to produce simpler oligosaccharides. A previous report suggested that xylanase could be useful in enhancing the efficiency of biofuel production [2]. Other reviews about xylanase are also available in earlier publications [5–7].

As published online in the CAZy database, the GH families that correlate with xylanases include GH3, 5, 8, 9, 10, 11, 12, 16, 26, 30, 43, 44, 51, 62, 98, and 141. In among these families, GH10 (formerly known as family F) and GH11 (family G) xylanases are the well-studied groups. The GH10 xylanases have a broader range of substrate hydrolyzing ability, where some of the members can hydrolyze compounds such as β-glucan, *p*-nitrophenol-β-cellobiose, and carboxymethyl cellulose [3]. GH10 xylanases consist of a typical $(\beta/\alpha)_8$ TIM-barrel fold and are characterized by a relatively low pI and have higher molecular mass [4]. Xylanases associated to GH11 have higher specificity toward xylan than that of GH10 [5]. They adopt β-jelly rolls structure, exhibit higher pI, and lower molecular mass [6].

Rhodothermaceae bacterium RA is a halo-thermophile that was isolated from a hot spring [7]. The complete genome of this bacterium had been reported and the result suggested that this bacterium could be a new genus under *Rhodothermaceae* [8]. Although a total of 57 different GH sequences (including two GH10 xylanases) were found in its genome, none of these enzymes have been described biochemically. In this report, we investigated the enzyme properties of a xylanase from this bacterium.

* Corresponding author.
E-mail address: gohkianmau@utm.my (K.M. Goh).

https://doi.org/10.1016/j.pep.2019.105464
Received 25 February 2019; Received in revised form 10 June 2019; Accepted 31 July 2019
Available online 01 August 2019

2. Materials and methods

2.1. Media and chemicals

Marine Broth (MB) and Luria-Bertani (LB) media were purchased from Laboratorios Conda (Madrid, Spain). Kanamycin and isopropyl β-D-1-thiogalactopyranoside (IPTG) were purchased from Merck Millipore (Burlington, USA). DNeasy® Blood & Tissue Kit, QIAprep® Spin Miniprep Kit, QIAquick PCR & Gel Cleanup Kit, and Ni-NTA superflow column were purchased from Qiagen (Venlo, Netherlands). KAPA HiFi HotStart ReadyMix DNA polymerase, restriction enzymes (*Eco*RI and *Not*I), and Novagen® *p*ET28a-(+) expression vector were purchased from Kapa Biosystems (Wilmington, USA), New England Biolabs (Ipswich, USA), and Novagen (Madison, USA), respectively. The forward and reverse primers were synthesized by Integrated DNA Technologies (Coralville, USA). B-PER Direct Bacterial Protein Extraction Kit, Pierce™ BCA Protein Assay Kit, Imperial™ Protein Stain, and Benchmark™ Protein Ladder were purchased from Thermo Scientific (Waltham, USA). Beechwood xylan for the enzymatic assay was purchased from Megazyme (Bray, Ireland).

2.2. Microorganism and culture conditions

Rhodothermaceae bacterium RA (KCTC 62031) was used as the source for isolating xylanase gene [7,8], and it was grown in MB medium at 50 °C, pH 7 with agitation (200 rpm) for 48 h. *E. coli* BL21(DE3) was used as the bacterial host for the recombinant protein, and it was grown in LB medium at 37 °C, pH 7 with agitation (200 rpm) for 16 h.

2.3. Gene isolation and vector construction

The genome of *Rhodothermaceae* bacterium RA was extracted using a DNeasy® Blood & Tissue Kit. Gene amplification was carried out using KAPA HiFi HotStart ReadyMix DNA polymerase, with specific primers (5′-ATCCGAATTCGCCCCCGGCGAGGAGCCGGT-3′ and 5′- AGTGCGGCCGCCTCGCGCGCGGTGGCCACGAC-3′, the underlined sequences in the primers corresponding to restriction sites *Eco*RI and *Not*I, respectively). The polymerase chain reaction was conducted in a thermocycler, and the settings were initial denaturation at 95 °C for 5 min, then 30 cycles of (denaturation at 95 °C for 1 min, annealing at 55 °C for 30 s, and extension at 72 °C for 1 min), and final extension at 72 °C for 10 min. The amplified *XynRA1* gene product was cloned into the Novagen® *pET*28a-(+) expression vector, while the recombinant vector (*pET*28a-*XynRA1*) was transformed into *E. coli* BL21(DE3) strain for effective protein expression.

2.4. Expression of the xylanase gene

The cell harboring the constructed vector *pET*28a-*XynRA1* was grown in LB medium added with kanamycin (50 μg/mL) at 37 °C, pH 7 with 200 rpm agitation. When the culture reached the exponential phase (OD_{600nm} = 0.5–0.6), xylanase expression was induced by adding IPTG at a final concentration of 0.4 mM and incubated for another 3 h. After that, the bacteria cells were harvested by centrifugation at 4 °C, 5000 × *g* for 10 min and lysed by a B-PER Direct Bacterial Protein Extraction Kit to release the total protein.

2.5. Purification of the recombinant xylanase

Immobilized metal affinity chromatography (IMAC) technique was used to separate the xylanase XynRA1 from other proteins. The purification was carried out by injecting 1 mL of crude lysate into a Ni-NTA Superflow column connected to an ÄKTA Start chromatography system (GE Healthcare, Chicago, USA). The column resin was equilibrated with sodium phosphate buffer (20 mM, pH 7.4) containing 500 mM NaCl. The bound protein was eluted with the same buffer containing a linear gradient of imidazole (60–350 mM). The purified xylanase was dialyzed in sodium phosphate buffer (100 mM, pH 7.4) at 4 °C overnight.

2.6. Determination of enzyme activity and protein concentration

The xylanase activity was determined using 3,5-dinitrosalicylic acid (DNS) assay. Beechwood xylan was used as the substrate unless specified. The enzyme reaction was conducted by mixing 0.05 mL of purified XynRA1 and 0.5 mL of 1% (*w/v*) beechwood xylan in sodium phosphate buffer (100 mM, pH 8.0). After incubation at 60 °C for 15 min, the enzyme reaction was immediately stopped by adding 0.5 mL DNS solution. The mixture was then subjected to boiling for 5 min and quenched on ice for another 2 min. The absorbance changes were detected at OD_{540nm} in a spectrophotometer. One unit (U) of xylanase activity is defined as the amount of enzyme required to release 1 μmol of reducing sugars per min per mL under the assay condition.

The protein concentration of purified XynRA1 was quantified using Pierce™ BCA Protein Assay Kit. Both enzymatic and protein concentration assays were performed in at least triplicates.

2.7. Bioinformatics analyses of XynRA1

The protein sequence of XynRA1 was subjected to various analyses such as InterProScan, ProtParam, Signal-Blast, TMHMM Server v. 2.0, and ScanProsite [9–13]. The sequences of GH10 xylanases from different microorganisms were retrieved using the Carbohydrate-Active Enzyme (CAZy) database. The relationship of XynRA1 with other GH10 xylanases was analyzed by a maximum-parsimony phylogenetic tree. The positions of the motifs in XynRA1 were determined by referring to the SPRINT database. A Weblogo online generator was used to differentiate the motif sequences among the GH10 xylanases [14].

2.8. Characterization of XynRA1

2.8.1. Gel electrophoresis and zymogram

Both crude and purified enzymes of XynRA1 were subjected to sodium dodecyl sulfate-polyacrylamide gel electrophoresis (SDS-PAGE). The denaturing gel used was 5% (*w/v*) stacking gel and 12% (*w/v*) resolving gel. Upon loading the protein samples into the gel, electrophoresis was conducted at 150 V for 55 min. Imperial™ Protein Stain was used to stain the protein bands, and the molecular weight of the bands was compared with Benchmark™ Protein Ladder.

Zymography of the purified XynRA1 was carried out by SDS-PAGE as described above. Upon electrophoresis, the gel was washed with 10% (*v/v*) Triton-X 100 for 30 min to remove the remaining SDS. The gel was then incubated in 1% (*w/v*) beechwood xylan solution for 1 h to allow the diffusion of the substrates into the gel. To maximize the enzymatic reaction, the gel was immersed in 100 mM sodium phosphate buffer (pH 8) and incubated at 60 °C for 24 h. The gel was then stained using 0.1% (*w/v*) congo red for 30 min, followed by destaining using 1 M NaCl solution.

2.8.2. Effects of temperature and pH

Enzyme reactions were conducted at different temperatures (20–90 °C) and pH (pH 2–11) for 15 min to determine the optimum temperature and pH of XynRA1. The buffers used in this test included glycine-HCl (pH 2–3), sodium acetate (pH 4–5), sodium phosphate (pH 6–7.5), Tris-HCl (pH 8–9), and carbonate-bicarbonate (pH 9.5–11) buffers. Thermostability of XynRA1 was conducted by incubating the enzyme at various temperatures (50 °C, 60 °C, and 70 °C), without any substrate added. At a specific time interval, samples were collected from the preincubated enzyme and subjected to enzymatic reactions. A plot of residual activity versus time was used to elaborate the thermostability of the enzyme. The test was conducted in at least triplicate.

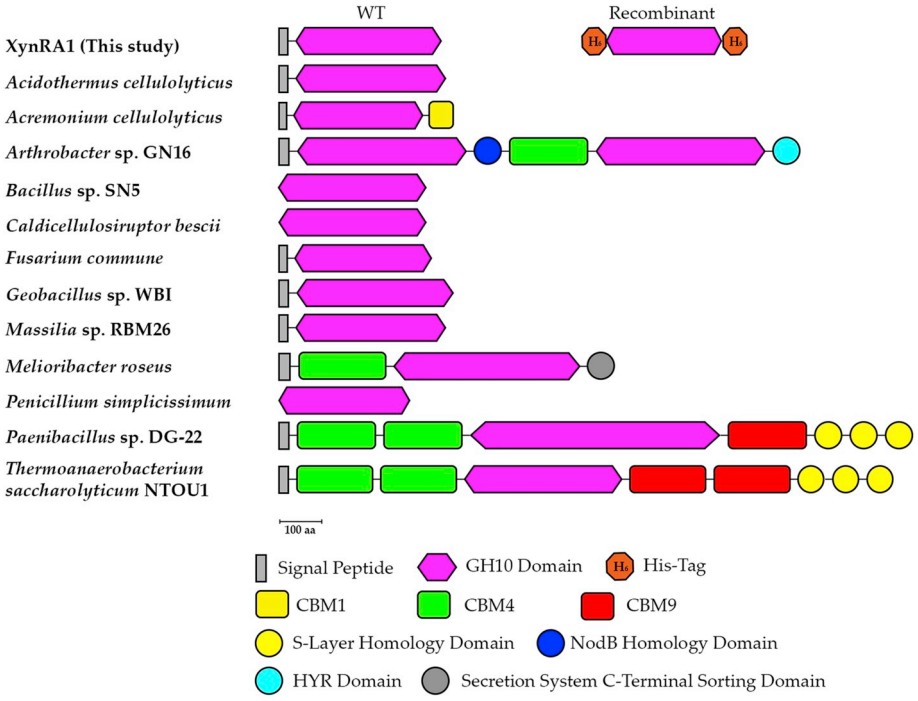

Fig. 1. The structural differences between XynRA1 with other characterized GH10 xylanases. XynRA1 adopt a simpler architecture in its domain arrangement.

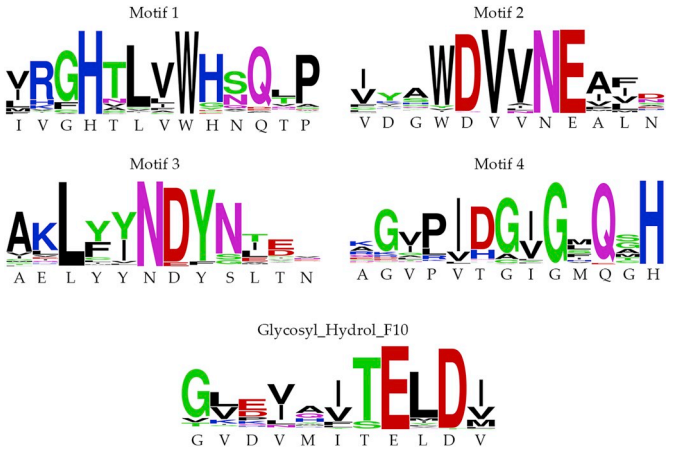

Fig. 2. The consensus motifs and Glycosyl_Hydrol_F10 of XynRA1 with other 220 GH10 xylanases. The sequence of XynRA1 was shown below the Weblogo. The SPRINT accession number for motifs 1–4 and Glycosyl_Hydrol_F10 are PR00134 and PS00591, respectively. All the motif sequences of XynRA1 are highly similar as compared to the motifs from other GH10 xylanases.

2.8.3. Effects of metal ions and chemical reagents

The purified XynRA1 was subjected to standard enzymatic reactions carried out at 60 °C and pH 8 with supplementation of different types of salt at 5 mM concentration (eg. $CaCl_2$, NaCl, KCl, $MgCl_2$, $FeCl_3$, $NiCl_2$, $CoCl_2$, NH_4Cl, $ZnSO_4$, $MnSO_4$, $CuSO_4$, RbCl, $SrCl_2$, and $BaCl_2$) or different chemical reagents at 5% (*v/v*) (eg. urea, SDS, EDTA, Tween-20, Tween-40, Tween-60, Tween-80, Triton X-100, and DMSO). The relative activity of each reaction was calculated against the non-salt/chemical supplemented reference. The test was conducted in at least triplicate.

2.8.4. Salt tolerance

The purified XynRA1 was subjected to a salinity test by conducting the enzymatic reactions in the presence of NaCl at various concentrations (0–3.0 M). Enzyme activity at 0 M NaCl was used as the reference for relative activity calculation. The test was conducted in at least triplicate.

2.8.5. Kinetic parameter

The purified XynRA1 was subjected to enzyme kinetic analysis by conducting the enzyme assay at optimum temperature and pH, with different concentration of beechwood xylan provided, ranging from 0.2 to 6.0 mg/mL. Each of the data points was collected in at least triplicates. K_m, V_{max}, and k_{cat} values of the enzyme were determined using the GraphPad Prism 7 software.

2.8.6. HPLC analysis

The post-reaction products from the enzyme assays were analyzed by an Agilent 1260 Infinity high-performance liquid chromatography (HPLC) system (Agilent Technologies, Santa Clara, USA). An Agilent 385-Evaporative Light Scattering Detector was used to detect the presence of simple sugars. A Rezex RSO-Oligosaccharide Ag^+ column (Phenomenex Inc, Torrance, USA) was used to separate the sugar mixture. The mobile phase used was ultrapure water. The HPLC setting used were 0.2 mL/min flow rate and 80 °C column temperature. The ELSD setting used were 30 °C evaporator temperature, 30 °C nebulizer temperature and 1.6 SLM evaporator gas flow. All the analyses were triplicated.

3. Results and discussions

3.1. Bioinformatics analyses of xynRA1

This team previously reported the genome analysis of *Rhodothermaceae* bacterium RA [8]. Genome mining revealed that this bacterium consists of 17 genes that are important for both cellulolytic and hemicellulolytic activities. Among these genes, *xynRA1*, a gene with the size of 1140 bp that encodes xylanase with 379 amino acids, was selected for further study. This gene was deposited in Genbank with the locus-tag of **AWN76_008205**, and its translated protein was deposited as **ARA95075.1**.

None of the well-studied xylanases share close sequence similarity to that of XynRA1. At the time of writing, the closest protein sequence to XynRA1 are xylanases from *Gemmatimonadetes* spp. (57.2–65.4% in similarity), *Candidatus solibacter usitatus* (61.8%), *Rubrivirga marina* (60.7%), *Acidobacteria* (58.9–61.0%), *Ignavibacteria* bacterium

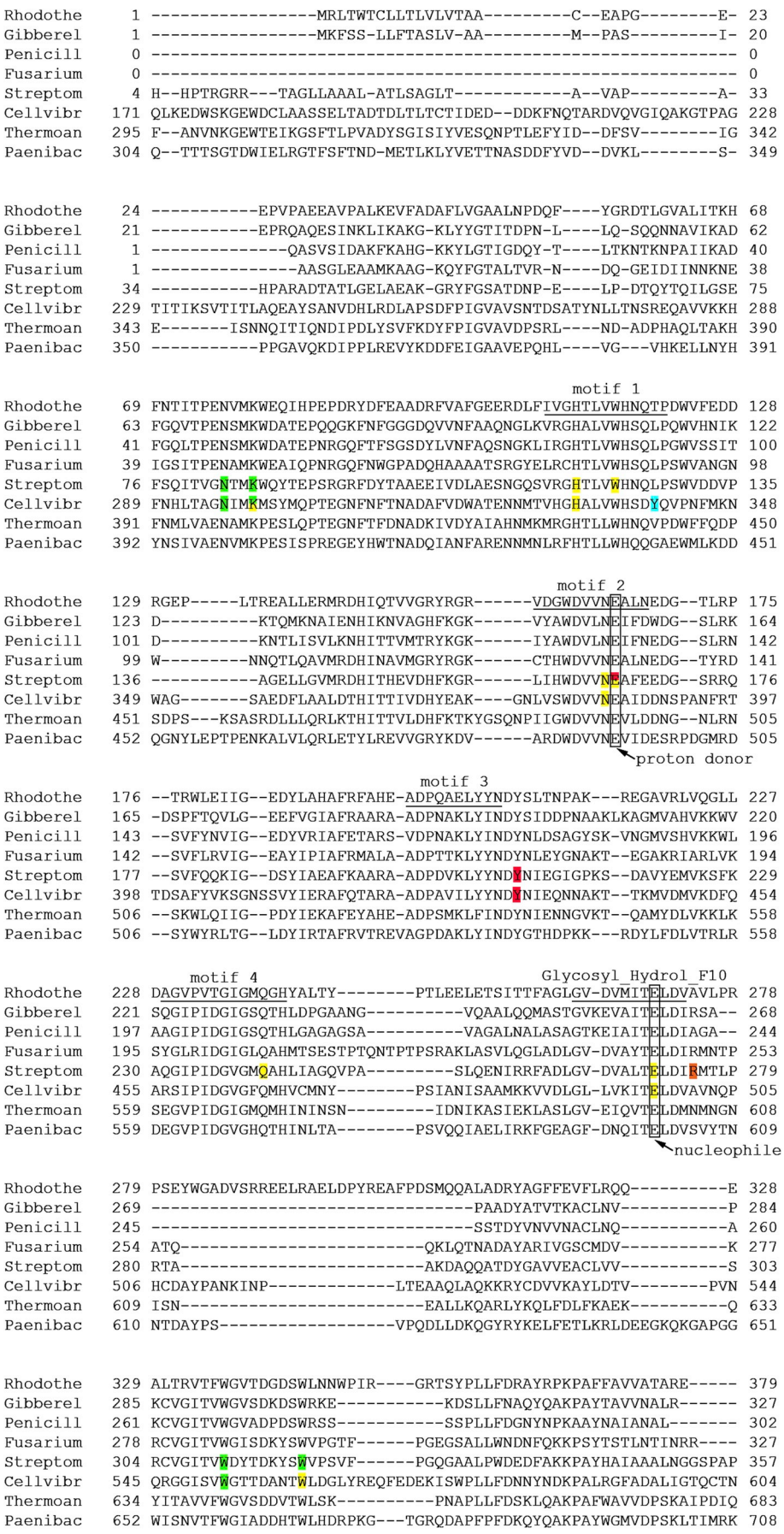

Fig. 3. Multiple sequence alignment of XynRA1 with GH10 xylanases from various sources. Abbreviation: Rhodothe: *Rhodothermaceae* bacterium RA XynRA1 (this study), Gibberel: *Gibberella zeae* (Uniprot ID: I1S3T9), Penicill: *Penicillium simplicissimum* (P56588, PDB ID: 1B30, 1B31, 1B3V, 1B3W, 1B3X, 1B3Y, 1B3Z, and 1BG4), Fusarium: *Fusarium oxysporum f.* sp. *lycopersici* (B3A0S5, 3U7B), Streptom: *Streptomyces* sp. (B4XVN1, 3WUB, 3WUE, 3WUF, and 3WUG), Cellvibr: *Cellvibrio japonicus* (Q59675, 1GNY, 1US2, and 1US3), Thermoan: *Thermoanaerobacterium saccharolyticum* (P36917), and Paenibac: *Paenibacillus* sp. DG-22 (A0A075EEX4). The catalytic residues of XynRA1 were predicted as E165 and E270 (as shown in the box). The underlined sequences are the location of the motifs for XynRA1. Amino acids shown in blue (subsite −3), green (subsite −2), yellow (subsite −1), red (subsite +1), and orange (subsite +2) background are the locations of subsites as shown in the GH10 xylanase structures of *Streptomyces* sp. and *Cellvibrio japonicus*. The amino acid residues of these subsites were also conserved in the sequence of XynRA1, suggesting that XynRA1 may harbor the same subsites for substrate binding.

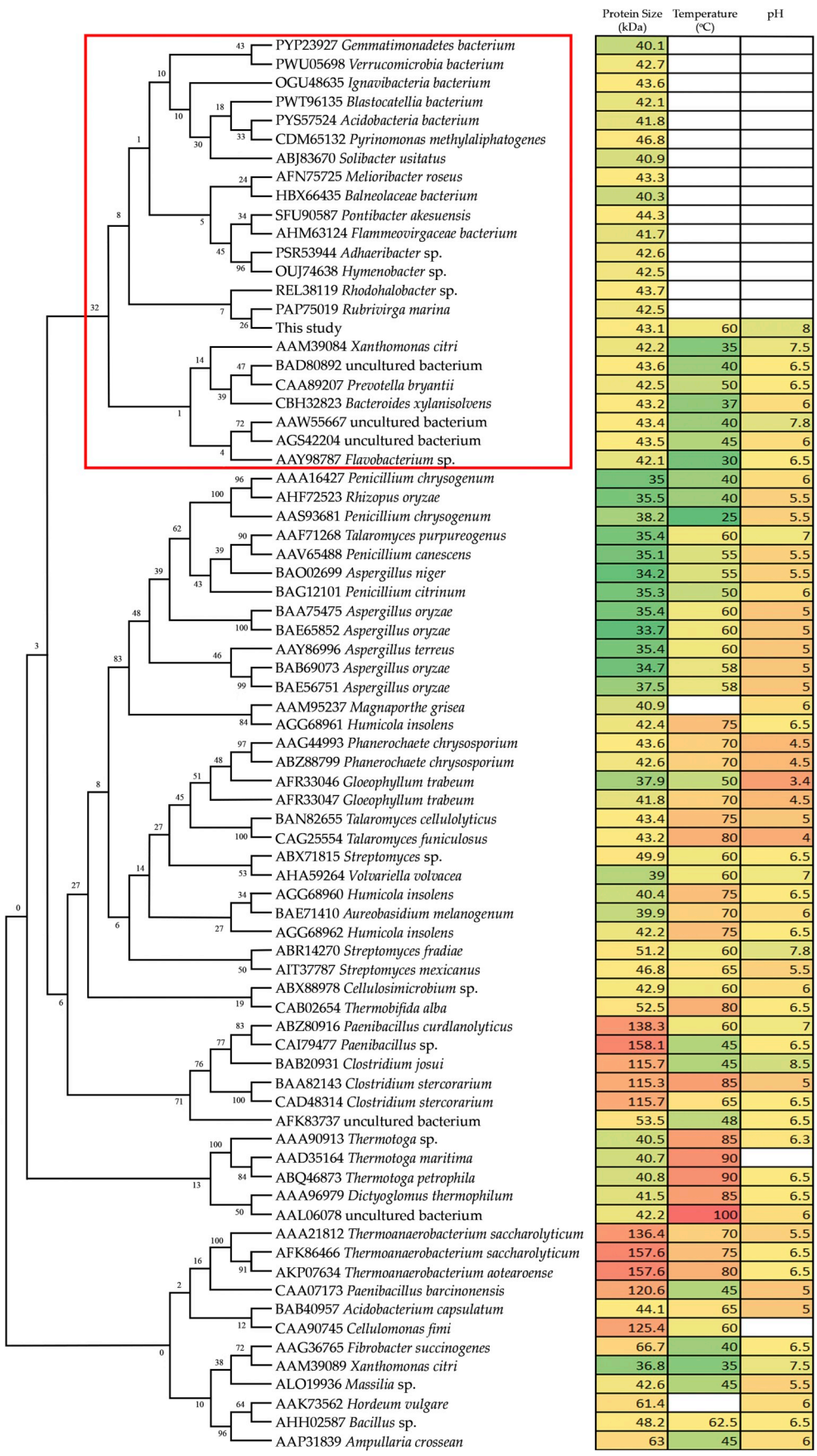

Fig. 4. Phylogenetic analysis of XynRA1 with other biochemically characterized GH10 xylanases. The maximum-parsimony (MP) tree was constructed using MEGA X program. The tree constructed was undergone verification with the bootstrap test (1000 replicates) and the value shown beside the branches of the tree indicates the percentage of replicate from the test. The tree (left) was correlated with three enzyme properties (right) – protein size, optimum temperature, and optimum pH. The color changes are from Green – Yellow – Red, indicating the values increment of each factor. The red box represented the grouping of XynRA1 with other closer GH10 xylanases. XynRA1 clustered with GH10 xylanases of similar size (40–44 kDa), and it has the highest optimum temperature and pH among them.

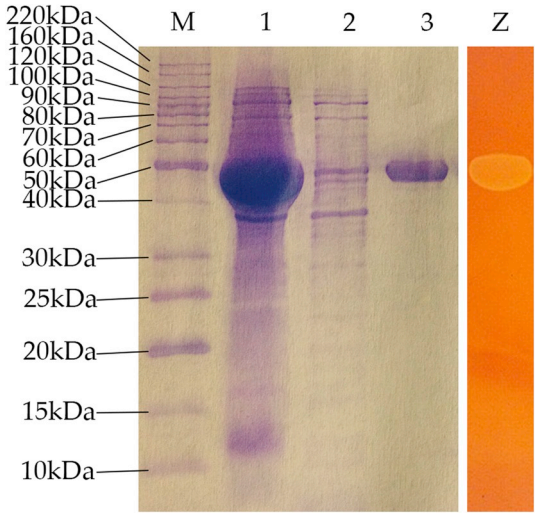

Fig. 5. SDS-PAGE and zymogram of purified XynRA1. Lane M: Molecular weight standard; lane 1: crude lysate; lane 2: flowthrough from purification step; lane 3: recombinant XynRA1; lane Z: Zymography analysis of XynRA1 with substrate beechwood xylan. The molecular weight of the purified XynRA1 is approximately 49 kDa.

GWB2_36_8 (60.9%), *Pyrinomonas methylaliphatogenes* (60.9%), and *Blastocatellia* (59.8%). The function and biochemical characterization of the proteins as mentioned above are yet to be determined as these genes were putatively annotated from the several whole-genome sequencing projects. In comparison to characterized xylanases from *Flavobacterium* sp. MSY2, *Xanthomonas citri* 306, and *Bacteroides xylanisolvens* XB1A, these enzymes shared an average sequence similarity of 47.0% to XynRA1 [15–17]. Moreover, another GH10 xylanase (namely Xyn10J), which was cloned from a compost metagenomic library, had also been characterized, and this Xyn10J shared sequence similarity of 46.1% to XynRA1 [18].

Based on the InterProScan analysis, the XynRA1 consists of a GH10 family domain and a signal peptide sequence (amino acid position 1–23) at the N-terminal (Fig. 1). The transmembrane region was absent as predicted using TMHMM Server v. 2.0. Collectively, wild type *Rhodothermaceae* bacterium RA expresses XynRA1 as an extracellular enzyme. Fig. 1 illustrates the domain architecture of XynRA1 and other selected GH10 xylanases. Some xylanases exhibited a relatively shorter length of protein sequence and contained only a single domain, which was the catalytic domain. Examples of these xylanases included those initially produced by *Bacillus* sp. SN5, *Caldicellulosiruptor bescii*, and *Penicillium simplicissimum*, and were expressed intracellularly in the wild type organism [19–21]. XynRA1 and other xylanases such as the one secreted by *Acidothermus cellulolyticus* also exhibited a single catalytic domain but was expressed extracellularly due to the presence of a signal peptide [22]. Certain xylanases grouped in GH10 superfamily contain more complex domains arrangement; these include proteins found initially in *Arthrobacter* sp. GN16, *Melioribacter roseus*, *Paenibacillus* sp. DG-22, and others [23–25]. To the best of the researchers' knowledge, a xylanase from *Thermoanaerobacterium saccharolyticum* NTOU1 had the most complicated domain setup (Fig. 1). Other information about GH10 multidomain xylanase can be found elsewhere [26–30]. For other GH families such as the GH13 (α-amylase) is further subdivided into subfamilies due to vast diversity [31]. To date, GH10 remains as a single division although xylanases are very diverse in sequence as well as domains arrangement (Fig. 1). The subfamily classification for GH10 is needed for increasing the resolution of protein diversity.

Fig. 2 is a Weblogo representation of currently known motif using 228 GH10 xylanases sequences. Motifs 1–4 are recognition fingerprints for GH10 family. An active site motif, namely Glycosyl_Hydrol_F10 was present in the XynRA1 as well. As reported in PROSITE, the pattern of this active site motif is [GTA]-{QNAG}-{GSV}-[LIVN]-x-[IVMF]-[ST]-E−[LIY]-[DN]-[LIVMF]. It is a stretch of peptides formed by 11 amino acids. Fig. 3 shows the multiple sequence alignment of XynRA1 with another six GH10 xylanases. Information like motifs, active sites, and subsites are presented in the same figure. Based on the alignment, the active site of XynRA1 was predicted as E165 (proton donor) and E270 (nucleophile). Subsites of GH10 xylanases had been summarized recently based on 19 GH10 xylanases with the crystal structures, and it was reported that these enzymes could have up to 6 subsites (subsite −3 to +3) with 17 amino acid residues interacting with the substrate [32]. Please refer to Supplementary Table 1 for the locations of the predicted subsites for XynRA1.

The relationship between GH10 xylanases and XynRA1 was analyzed by a maximum-parsimony tree (Fig. 4). Only biochemically characterized enzymes were included in the tree unless specified. XynRA1 falls into a cluster with xylanases from mostly mesophilic bacteria such as *Rubrivirga marina*, *Solibacter usitatus*, and *Flavobacterium* sp. MSY2. Within this cluster, only xylanases from *Ignavibacteria* bacterium GWC2_36_12, *Melioribacter roseus*, and *Rhodothermaceae* bacterium RA (XynRA1) are thermophilic origins. All the members in this big cluster have a similar protein size, which is between 40 and 44 kDa. Moreover, XynRA1 has the highest optimum temperature and pH among the members in the cluster based on the existing biochemical data.

3.2. Characterization of purified XynRA1

Fig. 5 illustrates both the results from SDS-PAGE and zymography. The recombinant XynRA1 has an apparent molecular weight of approximately 49 kDa, which corresponded with the calculated protein size of 46.7 kDa. The theoretical pI value of the enzyme is 4.64. Table 1 summarizes the characteristic of XynRA1 and the comparison to other commonly known xylanases. XynRA1 is relatively small in size in comparing to many xylanases. The smallest GH10 xylanase recorded to date is from *P. simplicissium*, which is around 32.6 kDa [21]. For larger xylanases, the size increment is due to the presence of multidomains as described in the earlier section.

As shown in Fig. 6a, recombinant XynRA1 had an optimum temperature of 60 °C, and it can retain more than 60% of its maximal activity at a temperature ranging from 50 °C to 70 °C. As compared with other xylanases (Table 1), this characteristic is similar to GH10 xylanases initially identified in *Streptomyces coelicolor* A3(2), *Microbacterium trichothercenolyticum* HY-17, as well as a xylanase cloned from the environmental DNA of a paper mill [30,33,34]. These enzymes achieved optimal activity at around 60 °C as well.

Moreover, the enzyme showed an absolute peak at pH 8, and it can maintain more than 50% of its maximal activity at a pH range from 6.5 to 9.5 as shown in Fig. 6b. When the pH exceeded the range, the activity of the enzyme dropped significantly, achieving less than 10% of its maximum value. Most of the GH10 xylanases found recently were working in acidic or neutral condition (Table 1); there were very few of the candidates that functioned in alkaline condition, except the xylanase from *Microcella alkaliphile* [35] that had the optimum of pH 8, *M. trichothercenolyticum* HY-17 (pH 9) [34], *Geobacillus* sp. WBI (pH 6–9) [36], and *Paenibacillus* sp. strain E18 (pH 7.5–9) [37].

Fig. 6c illustrates the salt tolerance ability of XynRA1. Although XynRA1 originates from a halo-thermophile, this protein does not inherit the ability to withstand high NaCl concentration. XynRA1 activity dropped half when the NaCl concentration increased to 0.6 M (salinity of seawater is ~0.6 M). At NaCl concentration higher than 0.6 M, its activity gradually decreased. As described by DasSarma and DasSarma [38], the factors that allow the protein to function at high salinity include the solvation ability of the enzyme, the increment in ion-pair networks, reduction of hydrophobic surface patches, and an unusually high number of ordered side chains in the protein. Examples of bacteria

Table 1
Properties of GH10 xylanases from various microorganisms.

Origin	Source	MW (kDa)	Opt. temp. °C	Opt. pH	Thermostability	K_m (mg/mL)[a]	V_{max} (μmol/min/mg)[b]	Ref
Rhodothermaceae bacterium RA	bacteria	43.1	60	8	$t_{1/2}$ at 60 °C = 1 h	1.36	1214	this study
Acidothermus cellulolyticus 11B	bacteria	47.0	90	6	$t_{1/2}$ at 90 °C = 1 h 30 min	0.53	350	[22]
Acremonium cellulolyticus	fungus	51.0	70.5	5	ND	ND	ND	[43]
Arthrobacter sp. GN16	bacteria	131.5	45	5.5	$t_{1/2}$ at 50 °C = 2 min	2.6	65.4	[23]
Aspergillus nidulans	fungus		60	7.5	$t_{1/2}$ at 50 °C = 49 h $t_{1/2}$ at 60 °C = 20 min	1.66	193.3 μmol/min/mL	[41]
Bacillus sp. SN5	bacteria	45.0	40	7	$t_{1/2}$ at 40 °C = 30 min	0.6	114	[19]
Caldicellulosiruptor bescii	bacteria	40.2	70	7.2	$t_{1/2}$ at 60 °C = 7 h 42 min	1.90	ND	[20]
Compost metagenome (Xyn10J)		40.0	40	7	$t_{1/2}$ at 50 °C = 30 min	ND	ND	[18]
Fusarium commune (XYL10A)	fungus	35.7	50	6	ND	ND	ND	[44]
Fusarium commune (XYL10B)	fungus	39.3	50	6	ND	ND	ND	[44]
Genomic DNA from alkaline wastewater sludge of a paper mill		158.2	60	7	ND	1.01	73.53	[30]
Geobacillus sp. WBI	bacteria	47.0	70	6–9	ND	0.9	0.8	[36]
Glaciecolar mesophila KMM 241	bacteria	47.5	30	7	$t_{1/2}$ at 30 °C = 25 min	1.22	98.31	[40]
Massilia sp. RBM26	bacteria	45.0	45	5.5	$t_{1/2}$ at 55 °C = 7 min	9.49	65.79	[45]
Melioribacter roseus (Xyl2091)	bacteria	86.0	65	6.5	$t_{1/2}$ at 60 °C = 2 h 50 min	3	130.2	[24]
Melioribacter roseus (Xyl2495)	bacteria	42.0	40	6.5	$t_{1/2}$ at 70 °C = 1 h	1.05	3230.8	[24]
Metagenomic fosmid library of Hu sheep rumen contents	bacteria	71.3	50	6	$t_{1/2}$ at 50 °C = 9 min	4.39	3.2	[46]
Microbacterium trichothercenolyticum HY-17	bacteria	41.6	60	9	$t_{1/2}$ at 55 °C = 12 min	ND	ND	[34]
Microcella alkaliphile	bacteria	150.0	65	8	$t_{1/2}$ at 50 °C = 48 h	ND	ND	[35]
Paenibacillus curdlanolyticus	bacteria	45.0	35	7.5	ND	2	3.7	[47]
Paenibacillus sp. DG-22	bacteria	159.5	65	6.5	ND	3.49	201.34	[25]
Paenibacillus sp. HPL-001	bacteria	38.1	50	5.5	ND	5.35	199.17	[48]
Paenibacillus sp. strain E18	bacteria	37.8	50	7.5–9	ND	0.51	357.93 μmol/min/mL	[37]
Penicillium canescens	fungus	36.0	70	6	$t_{1/2}$ at 70 °C = 7 h	0.52	75	[49]
Penicillium funiculosum	fungus	41.0	70	5	ND	3.7	ND	[50]
Phialophora sp. G5	fungus	40.0	70	4	$t_{1/2}$ at 80 °C = 4 min	2.1	448.4	[51]
Phytophthora parasitica (PPXYN1)	fungus	65.5	40	6	$t_{1/2}$ at 100 °C = 90 min	ND	ND	[52]
Phytophthora parasitica (PPXYN2)	fungus	103.5	50	5	$t_{1/2}$ at 100 °C = 5 min	ND	ND	[52]
Phytophthora parasitica (PPXYN4)	fungus	64.3	30	6	$t_{1/2}$ at 100 °C < 5 min	ND	ND	[52]
Remersonia thermophila	fungus	42.0	65	6	$t_{1/2}$ at 50 °C = 35 min	2.477	5.787 μmol/min/mL	[53]
Saccharopolyspora pathumthaniensis S582	bacteria	36.0	70	6.5	$t_{1/2}$ at 60 °C = 3 h $t_{1/2}$ at 70 °C = 2 h	3.92	256	[42]
Streptomyces coelicolor A3(2)	bacteria	47.0	60	6	$t_{1/2}$ at 60 °C = 25 min	0.24	6.86	[33]
Thermoanaerobacterium saccharolyticum NTOU1	bacteria	154.0	70–73	5–7	ND	ND	ND	[39]
Thermotoga thermarum	bacteria	40.0	80	6	$t_{1/2}$ at 80 °C = 45 min	1.8	769	[54]
Thielavia terrestris Co3Bag1	fungus	82.0	85	5.5	$t_{1/2}$ at 65 °C = 23.1 days	0.41	21.52	[55]

*ND = Not Determined.

that produce high NaCl tolerance GH10 xylanases are *T. saccharolyticum* NTOU1, *Bacillus* sp. SN5, and *Glaciecolar mesophila* KMM 241, with the highest tolerance of 1.0 M, 1.3 M, and 2.1 M NaCl, respectively [19,39,40]. Their activities remained 100% at the stated concentration, and salt-activation occur at the NaCl concentration ranging from 0 to 0.5 M.

Fig. 6d displays the thermostability examination of XynRA1. Based on the results, the half-life of the recombinant XynRA1 enzyme was 1 h at 60 °C. When the pre-incubation was carried out at 50 °C, the enzyme retained 80% of its maximal activity for 5 h. The protein was unstable at 70 °C (Fig. 6d). Examples of GH10 xylanases that remain stable at 60 °C are those from *Aspergillus nidulans*, *C. bescii*, *M. roseus*, *Saccharopolyspora pathumthaniensis S582*, and *S. coelicolor* A3(2), with a half-life ranging from 20 min to 7.7 h [20,24,33,41,42].

Fig. 6e illustrates the Michaelis-Menten plot of XynRA1 where the reaction was carried out at its optimal temperature and pH with substrate beechwood xylan. The K_m, V_{max}, and k_{cat} values of XynRA1 were determined to be 1.36 ± 0.08 mg/mL, 1214 ± 26.01 U/mg, and 33.72 ± 0.72 s^{-1}, respectively. Table 1 summarizes the comparison of XynRA1 characteristics with other GH10 xylanases.

Table 2 shows the effects of metal ions and chemical reagents on XynRA1 activity. Overall, none of these supplemented compounds had positive effects on XynRA1. The relative activity of XynRA1 was 85% when 5 mM Na^+ was supplemented in the reaction tube. Similarly, the addition of other metal ions and chemical reagents significantly obstructed the XynRA1 enzyme activity, in particular, Fe^{3+}, Co^{2+}, Zn^+, Cu^{2+}, and SDS. The inhibition effects of metal ions like Mn^{2+}, Ag^{2+}, Fe^{2+}, Cu^{2+}, Hg^{2+}, Co^{2+}, and Pb^{2+} on other xylanases have long been reported [56]. However, very few of the xylanase candidates behaved like XynRA1, which exhibited extreme sensitivity against multiple metal ions. An example of xylanase that acts like XynRA1 is Xyn10G5 from *Phialophora* sp. G5 [51]. The author reported that the addition of Ag^+ and Hg^{2+} completely inhibited Xyn10G5, and slightly inhibited by other metal ions like Na^+, K^+, Li^+, Ca^{2+}, Mg^{2+}, and Mn^{2+} [51]. Xylanase from *Bacillus* sp. KT12 was also strongly inhibited by many types of metal ions, including Ca^{2+}, Mn^{2+}, Ba^{2+}, Co^{2+}, Mg^{2+}, Zn^{2+}, Cu^{2+}, and Fe^{2+} [57].

Theoretically, the following reasons attributed to protein inhibitions. a) Heavy metals, for example, Group IIb metals exhibit high affinity towards reactive groups like SH, $CONH_2$, NH_2, COOH, and PO_4 [58]. b) Heavy metals bound to the specific pocket may oxidize indole rings of tryptophan hence alter the biochemical function of the enzyme [59]. c) Alternatively, metal ions catalyse the cysteine thiol group autooxidation, which leads to the formation of intra- and intermolecular disulphide bonds or the formation of sulfenic acid [60]. Other than that, bivalent cations like Ca^{2+} and Mg^{2+} are activators for some of the

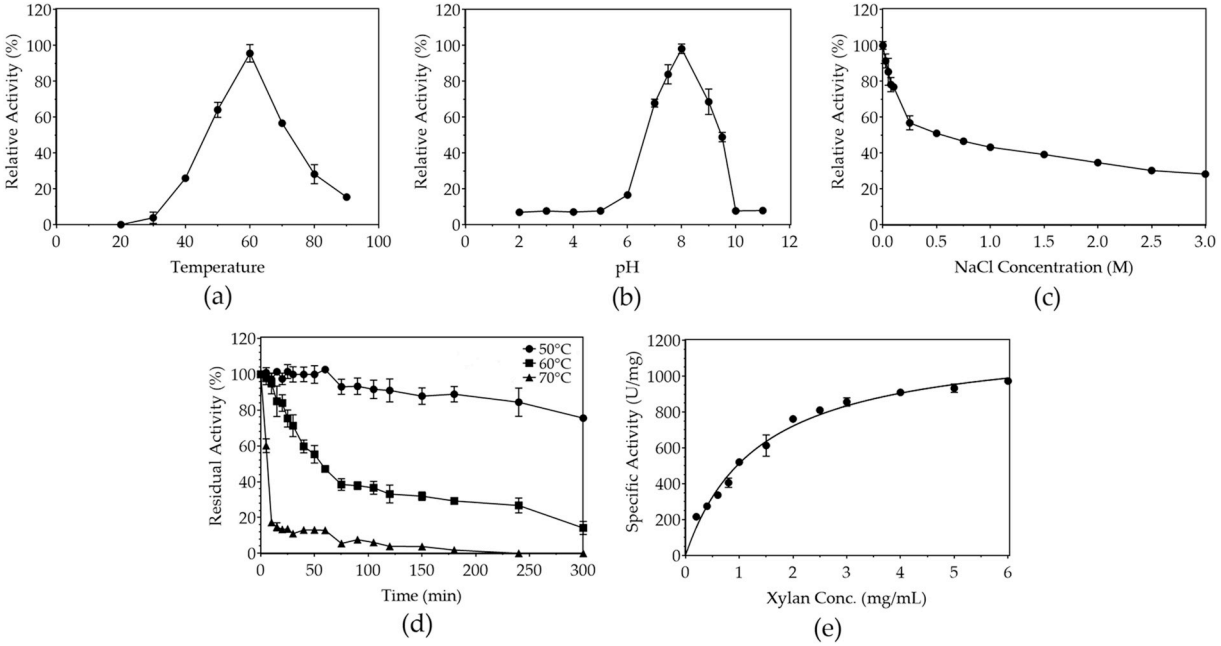

Fig. 6. Enzymatic characterization of XynRA1. (a) Effect of temperature on enzyme. (b) Effect of pH on the activity of XynRA1. (c) Effect of NaCl to XynRA1 activity. (d) Thermostability of XynRA1. (e) Nonlinear Michaelis-Menten plot of XynRA1 reacted against beechwood xylan. XynRA1 achieved optimal activity at 60 °C and pH 8. XynRA1 is NaCl intolerant. The half-life of XynRA1 was 1 h at 60 °C. The kinetic parameters (K_m, V_{max}, and k_{cat}) of XynRA1 were 1.36 ± 0.08 mg/mL, 1214 ± 26.01 U/mg, and 33.72 ± 0.72 s^{-1}, respectively.

Table 2
Effects of metal ions and chemical reagents to the activity of XynRA1.

Metal ions/Chemical reagents	Concentration	Relative activity (%)
Reference	0 mM	100.00 ± 0.0
Calcium Chloride	5 mM	47.42 ± 0.62
Sodium Chloride	5 mM	85.16 ± 0.79
Potassium Chloride	5 mM	32.22 ± 0.59
Magnesium Chloride	5 mM	45.47 ± 2.54
Iron (III) Chloride	5 mM	1.83 ± 1.19
Nickel (II) Chloride	5 mM	11.57 ± 0.93
Cobalt (II) Chloride	5 mM	3.27 ± 1.42
Ammonium Chloride	5 mM	56.83 ± 1.95
Zinc Sulfate	5 mM	0.00 ± 0.28
Manganese Sulfate	5 mM	14.48 ± 6.53
Copper (II) Sulfate	5 mM	0.00 ± 0.51
Rubidium Chloride	5 mM	58.33 ± 5.59
Strondium Chloride	5 mM	31.14 ± 2.21
Barium Chloride	5 mM	34.02 ± 0.82
Urea	5 mM	75.59 ± 5.65
SDS	5 mM	5.23 ± 7.78
EDTA	5 mM	15.69 ± 1.41
Tween-20	5%	63.73 ± 5.81
Tween-40	5%	50.83 ± 8.21
Tween-60	5%	63.22 ± 9.31
Tween-80	5%	60.13 ± 4.77
Triton X-100	5%	64.70 ± 4.12
DMSO	5%	77.87 ± 3.61

GH10 xylanases because these cations stabilize the enzyme-substrate complex [4,61,62]. However, in this study, XynRA1 was moderately inhibited by calcium chloride and magnesium chloride (Table 2). In a separate report by Hwang et al. [48], the GH10 xylanase from *Paenibacillus* sp. HPL-001 was also inhibited strongly by calcium chloride and magnesium chloride. The authors suspected that the inhibition was due to the presence of a metal binding site adjacent to the xylanase catalytic region that caused a protein conformational change [48].

HPLC analysis (Table 3 and Fig. 7a) elucidated that XynRA1 can hydrolyze beechwood xylan, oat spelt xylan, *Palmaria palmata* xylan, xylotriose, xylotetraose, xylopentaose, and xylohexaose. XynRA1 has a

Table 3
Hydrolysis of various substrates by purified XynRA1.

Substrates	Substrate depletion (%)
Beechwood xylan	61.05 ± 0.45
Oatspelt xylan	59.65 ± 1.38
Palmaria palmata xylan	96.57 ± 1.10
Xylobiose	6.22 ± 1.72
Xylotriose	100 ± 0.02
Xylotetraose	97.59 ± 0.08
Xylopentaose	98.46 ± 0.64
Xylohexaose	96.27 ± 0.59

Note.
The concentration of all the substrates used in the assay was 10 mg/mL.
Substrate depletion (%) $= \frac{Initial\ amount\ of\ substrate - final\ amount\ of\ substrate}{Initial\ amount\ of\ substrate} \times 100\%$
Data presented are the means value of three independent experiments.

very low efficiency towards xylobiose and cannot hydrolyze other substrates like Avicel, carboxymethyl cellulose (CMC), sigmacell cellulose, alpha-cellulose, pullulan, starch, chitin, cellooligosaccharides (cellobiose – celloheptaose), beta-gentibiose, lactose, maltose, salicin, and sucrose (data not shown). Fig. 7b illustrates the product profile of enzyme reaction against beechwood xylan at different incubation periods. In the first 15 min reaction, the predominantly formed products were xylobiose and xylotriose. The peak corresponding to xylose was negligible at the early stage. After an hour, the decreasing of xylotriose coincided with the increasing amount of xylobiose. After 5 h of reaction, the initially observed peak corresponding to xylotriose was nonextant, and this suggests that XynRA1 can saccharify xylotriose. In a prolonged reaction, an insignificant amount of xylose was observed. Collectively, the hydrolysis pattern of XynRA1 is illustrated in Fig. 7c, where the substrate preferable for XynRA1 is: xylooligosaccharides (DP 3–6) > *Palmaria palmata* xylan > beechwood xylan > oat spelt xylan > xylobiose. The hydrolysis pattern of XynRA1 is similar to other reported xylanases such as *Paenibacillus* sp. DG-22 and *C. bescii* [20,25], where the enzymes were active against xylooligosaccharides with at least three xylose chain (i.e xylotriose), and the reaction generated xylobiose predominantly.

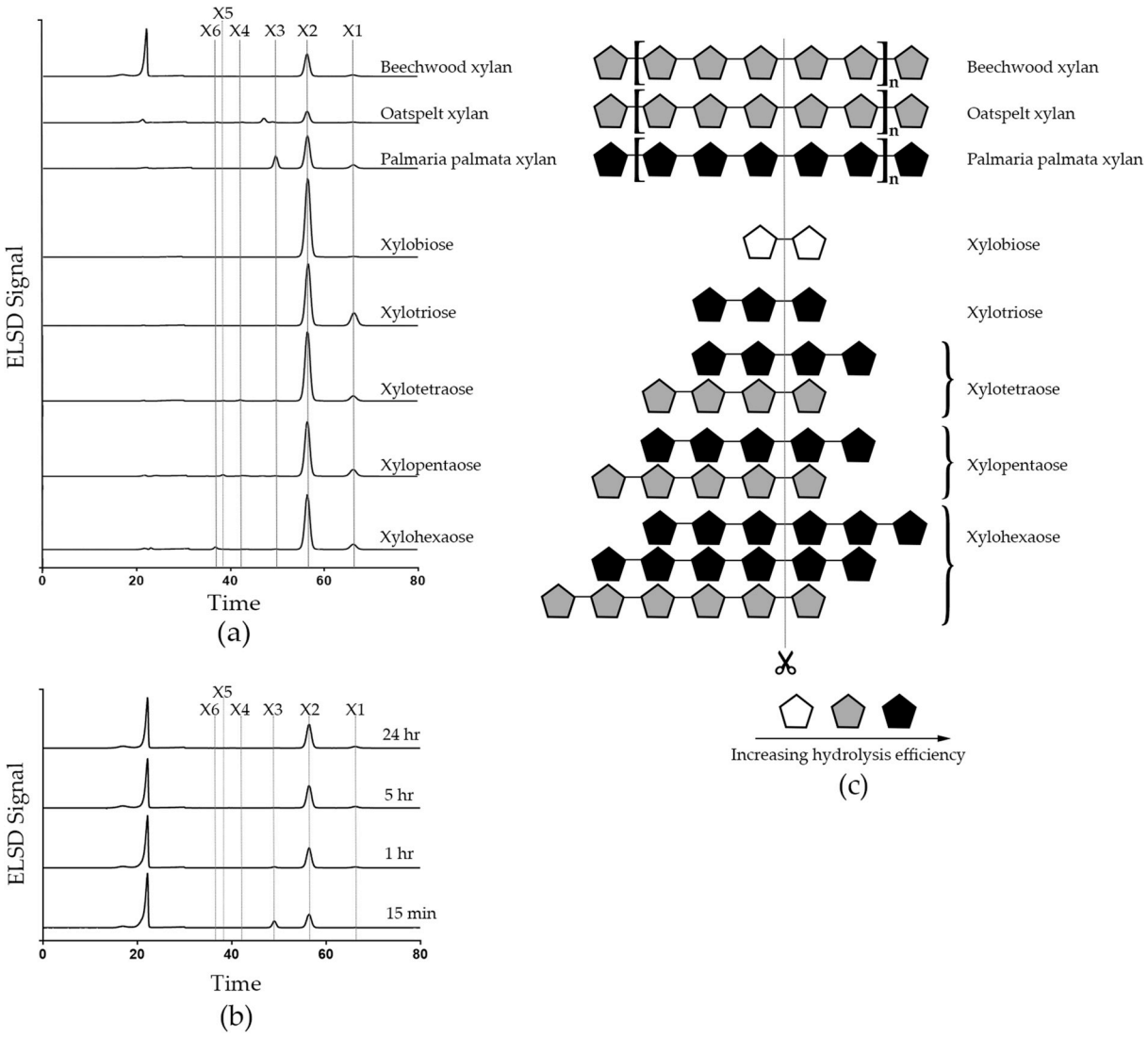

Fig. 7. HPLC analysis of the reaction products of XynRA1. (a) Enzymatic products of XynRA1 on various substrates after 24 h reaction. (b) Enzymatic products of XynRA1 on beechwood xylan after 15 min, 1 h, 5 h, and 24 h reactions. (c) The predicted hydrolytic ability of XynRA1 towards different substrates. X1–X6 (xylose–xylohexaose) represents the product peaks that were analyzed by the HPLC. The retention time for each of these product peaks was found to be 66 min, 56 min, 49 min, 43.5 min, 39 min, and 35.5 min, respectively. According to the analysis, the substrate preferable for XynRA1 is: xylooligosaccharides (DP 3–6) > *Palmaria palmata* xylan > beechwood xylan > oat spelt xylan > xylobiose.

An alkali and thermostable cellulase-free xylanase is useful to the paper and pulp industry, in particular for the biobleaching process that is carried out in alkali and high-temperature condition [63]. Besides, the enzyme might be helpful in alkali pretreatment of biomass for biofuel production.

4. Conclusion

In conclusion, the *xynRA1* gene from *Rhodothermaceae* bacterium RA was successfully cloned and expressed in *E. coli*. The recombinant protein was active in alkaline condition, remained stable at 50 °C up to 5 h and 60 °C for 1 h, sensitive to metal ions and NaCl, and yielded xylobiose as its main product. Based on the sequence analysis, XynRA1 represents xylanase that belongs to GH10. XynRA1 might be the right candidate for biobleaching process in the paper and pulp industry.

Conflicts of interest

The authors declare that there is no conflict of interest.

Acknowledgments

This work was supported by Universiti Teknologi Malaysia Research Grants (GUP Grant No. 16H89) and Newton Ungku Omar Fund (Grant No. 4B297, BB/P027717/1).

Appendix A. Supplementary data

Supplementary data to this article can be found online at https://doi.org/10.1016/j.pep.2019.105464.

References

[1] Y. Miao, J. Li, Z. Xiao, Q. Shen, R. Zhang, Characterization and identification of the xylanolytic enzymes from *Aspergillus fumigatus* Z5, BMC Microbiol. 15 (2015) 126.
[2] U.S.P. Uday, P. Choudhury, T.K. Bandyopadhyay, B. Bhunia, Classification, mode of action and production strategy of xylanase and its application for biofuel production from water hyacinth, Int. J. Biol. Macromol. 82 (2016) 1041–1054.
[3] J. Sermsathanaswadi, S. Baramee, C. Tachaapaikoon, P. Pason, K. Ratanakhanokchai, A. Kosugi, The family 22 carbohydrate-binding module of bifunctional xylanase/β-glucanase Xyn10E from *Paenibacillus curdlanolyticus* B-6 has an important role in lignocellulose degradation, Enzym. Microb. Technol. 96

(2017) 75–84.
[4] V. Juturu, J.C. Wu, Microbial xylanases: engineering, production and industrial applications, Biotechnol. Adv. 30 (2012) 1219–1227.
[5] T. Collins, C. Gerday, G. Feller, Xylanases, xylanase families and extremophilic xylanases, FEMS Microbiol. Rev. 29 (2005) 3–23.
[6] Y. Zheng, Y. Li, W. Liu, C.-C. Chen, T.-P. Ko, M. He, Z. Xu, M. Liu, H. Luo, R.-T. Guo, Structural insight into potential cold adaptation mechanism through a psychrophilic glycoside hydrolase family 10 endo-β-1, 4-xylanase, J. Struct. Biol. 193 (2016) 206–211.
[7] K.M. Goh, K.-G. Chan, S.W. Lim, K.J. Liew, C.S. Chan, M.S. Shamsir, R. Ee, T.-G.-S. Adrian, Genome analysis of a new *Rhodothermaceae* strain isolated from a hot spring, Front. Microbiol. 7 (2016) 1109.
[8] K.J. Liew, S.C. Teo, M.S. Shamsir, R.K. Sani, C.S. Chong, K.-G. Chan, K.M. Goh, Complete genome sequence of *Rhodothermaceae* bacterium RA with cellulolytic and xylanolytic activities, 3 Biotech 8 (2018) 376.
[9] P. Jones, D. Binns, H.-Y. Chang, M. Fraser, W. Li, C. McAnulla, H. McWilliam, J. Maslen, A. Mitchell, G. Nuka, InterProScan 5: genome-scale protein function classification, Bioinformatics 30 (2014) 1236–1240.
[10] E. Gasteiger, C. Hoogland, A. Gattiker, M.R. Wilkins, R.D. Appel, A. Bairoch, Protein identification and analysis tools on the ExPASy server, The Proteomics Protocols Handbook, Springer, 2005, pp. 571–607.
[11] K. Frank, M.J. Sippl, High-performance signal peptide prediction based on sequence alignment techniques, Bioinformatics 24 (2008) 2172–2176.
[12] A. Krogh, B. Larsson, G. Von Heijne, E.L. Sonnhammer, Predicting transmembrane protein topology with a hidden Markov model: application to complete genomes, J. Mol. Biol. 305 (2001) 567–580.
[13] E. De Castro, C.J. Sigrist, A. Gattiker, V. Bulliard, P.S. Langendijk-Genevaux, E. Gasteiger, A. Bairoch, N. Hulo, ScanProsite: detection of PROSITE signature matches and ProRule-associated functional and structural residues in proteins, Nucleic Acids Res. 34 (2006) W362–W365.
[14] G.E. Crooks, G. Hon, J.-M. Chandonia, S.E. Brenner, WebLogo: a sequence logo generator, Genome Res. 14 (2004) 1188–1190.
[15] C.C. Lee, M. Smith, R.E. Kibblewhite-Accinelli, T.G. Williams, K. Wagschal, G.H. Robertson, D.W. Wong, Isolation and characterization of a cold-active xylanase enzyme from *Flavobacterium* sp, Curr. Microbiol. 52 (2006) 112–116.
[16] C.R. Santos, Z.B. Hoffmam, V.P. de Matos Martins, L.M. Zanphorlin, L.H. de Paula Assis, R.V. Honorato, P.S.L. de Oliveira, R. Ruller, M.T. Murakami, Molecular mechanisms associated with xylan degradation by *Xanthomonas* plant pathogens, J. Biol. Chem. 289 (2014) 32186–32200.
[17] C. Mirande, P. Mosoni, C. Béra-Maillet, A. Bernalier-Donadille, E. Forano, Characterization of Xyn10A, a highly active xylanase from the human gut bacterium *Bacteroides xylanisolvens* XB1A, Appl. Biochem. Biotechnol. 87 (2010) 2097–2105.
[18] Y.S. Jeong, H.B. Na, S.K. Kim, Y.H. Kim, E.J. Kwon, J. Kim, H.D. Yun, J.-K. Lee, H. Kim, Characterization of Xyn10J, a novel family 10 xylanase from a compost metagenomic library, Appl. Biochem. Biotechnol. 166 (2012) 1328–1339.
[19] W. Bai, Y. Xue, C. Zhou, Y. Ma, Cloning, expression and characterization of a novel salt-tolerant xylanase from *Bacillus* sp. SN5, Biotechnol. Lett. 34 (2012) 2093–2099.
[20] J. An, Y. Xie, Y. Zhang, D. Tian, S. Wang, G. Yang, Y. Feng, Characterization of a thermostable, specific GH10 xylanase from *Caldicellulosiruptor bescii* with high catalytic activity, J. Mol. Catal. B Enzym. 117 (2015) 13–20.
[21] A. Schmidt, C. Kratky, A. Schlacher, H. Schwab, W. Steiner, Structure of the xylanase from *Penicillium simplicissimum*, Protein Sci. 7 (1998) 2081–2088.
[22] R.D. Barabote, J.V. Parales, Y.-Y. Guo, J.M. Labavitch, R.E. Parales, A.M. Berry, Xyn10A, a thermostable endoxylanase from *Acidothermus cellulolyticus* 11B, Appl. Environ. Microbiol. 76 (2010) 7363–7366.
[23] J. Zhou, J. Shen, R. Zhang, X. Tang, J. Li, B. Xu, J. Ding, Y. Gao, D. Xu, Z. Huang, Molecular and biochemical characterization of a novel multidomain xylanase from *Arthrobacter* sp. GN16 isolated from the feces of *Grus nigricollis*, Appl. Biochem. Biotechnol. 175 (2015) 573–588.
[24] A.L. Rakitin, A.Y. Ermakova, N.V. Ravin, Novel endoxylanases of the moderately thermophilic polysaccharide-degrading bacterium *Melioribacter roseus*, J. Microbiol. Biotechnol. 25 (2015) 1476–1484.
[25] S.H. Lee, Y.-E. Lee, Cloning and characterization of a multidomain GH10 xylanase from *Paenibacillus* sp. DG-22, J. Microbiol. Biotechnol. 24 (2014) 1525–1535.
[26] J.-X. Feng, S. Karita, E. Fujino, T. Fujino, T. Kimura, K. Sakka, K. Ohmiya, Cloning, sequencing, and expression of the gene encoding a cell-bound multi-domain xylanase from *Clostridium josui*, and characterization of the translated product, Biosci. Biotechnol. Biochem. 64 (2000) 2614–2624.
[27] Y. Ito, T. Tomita, N. Roy, A. Nakano, N. Sugawara-Tomita, S. Watanabe, N. Okai, N. Abe, Y. Kamio, Cloning, expression, and cell surface localization of *Paenibacillus* sp. strain W-61 xylanase 5, a multidomain xylanase, Appl. Environ. Microbiol. 69 (2003) 6969–6978.
[28] R. Waeonukul, P. Pason, K.L. Kyu, K. Sakka, A. Kosugi, Y. Mori, K. Ratanakhanokchai, Cloning, sequencing, and expression of the gene encoding a multidomain endo-β-1, 4-xylanase from *Paenibacillus curdlanolyticus* B-6, and characterization of the recombinant enzyme, J. Microbiol. Biotechnol. 19 (2009) 277–285.
[29] C. Winterhalter, P. Heinrich, A. Candussio, G. Wich, W. Liebl, Identification of a novel cellulose-binding domain the multidomain 120 kDa xylanase XynA of the hyperthermophilic bacterium *Thermotoga maritima*, Mol. Microbiol. 15 (1995) 431–444.
[30] Y. Zhao, K. Meng, H. Luo, H. Huang, T. Yuan, P. Yang, B. Yao, Molecular and biochemical characterization of a new alkaline active multidomain xylanase from alkaline wastewater sludge, World J. Microbiol. Biotechnol. 29 (2013) 327–334.
[31] M.R. Stam, E.G. Danchin, C. Rancurel, P.M. Coutinho, B. Henrissat, Dividing the large glycoside hydrolase family 13 into subfamilies: towards improved functional annotations of α-amylase-related proteins, Protein Eng. Des. Sel. 19 (2006) 555–562.
[32] B. Madan, S.-G. Lee, Sequence and structural features of subsite residues in GH10 and GH11 xylanases, Biotechnol. Bioproc. Eng. 23 (2018) 311–318.
[33] B. Enkhbaatar, C.-R. Lee, Y.-S. Hong, S.-K. Hong, Molecular characterization of xylobiose-and xylopentaose-producing β-1, 4-endoxylanase SCO5931 from *Streptomyces coelicolor* A3 (2), Appl. Biochem. Biotechnol. 180 (2016) 349–360.
[34] D.H. Shin, S. Jung, H.M. Kim, J.S. Lee, H.Y. Cho, K.S. Bae, C.K. Sung, Y.H. Rhee, K.H. Son, H.Y. Park, Novel alkali-tolerant GH10 endo-β-1, 4-xylanase with broad substrate specificity from *Microbacterium trichothecenolyticum* HY-17, a gut bacterium of the mole cricket *Gryllotalpa orientalis*, J. Microbiol. Biotechnol. 24 (2014) 943–953.
[35] K. Kuramochi, K. Uchimura, A. Kurata, T. Kobayashi, Y. Hirose, T. Miura, N. Kishimoto, R. Usami, K. Horikoshi, A high-molecular-weight, alkaline, and thermostable β-1, 4-xylanase of a subseafloor *Microcella alkaliphila*, Extremophiles 20 (2016) 471–478.
[36] S. Mitra, B.C. Mukhopadhyay, A.R. Mandal, A.P. Arukha, K. Chakrabarty, G.K. Das, P.K. Chakrabartty, S.R. Biswas, Cloning, overexpression, and characterization of a novel alkali-thermostable xylanase from *Geobacillus* sp. WBI, J. Basic Microbiol. 55 (2015) 527–537.
[37] P. Shi, J. Tian, T. Yuan, X. Liu, H. Huang, Y. Bai, P. Yang, X. Chen, N. Wu, B. Yao, *Paenibacillus* sp. strain E18 bifunctional xylanase-glucanase with a single catalytic domain, Appl. Environ. Microbiol. 76 (2010) 3620–3624.
[38] S. DasSarma, P. DasSarma, Halophiles and their enzymes: negativity put to good use, Curr. Opin. Microbiol. 25 (2015) 120–126.
[39] K.-S. Hung, S.-M. Liu, T.-Y. Fang, W.-S. Tzou, F.-P. Lin, K.-H. Sun, S.-J. Tang, Characterization of a salt-tolerant xylanase from *Thermoanaerobacterium saccharolyticum* NTOU1, Biotechnol. Lett. 33 (2011) 1441–1447.
[40] B. Guo, X.-L. Chen, C.-Y. Sun, B.-C. Zhou, Y.-Z. Zhang, Gene cloning, expression and characterization of a new cold-active and salt-tolerant endo-β-1, 4-xylanase from marine *Glaciecola mesophila* KMM 241, Appl. Biochem. Biotechnol. 84 (2009) 1107–1115.
[41] G.P. Maitan-Alfenas, M.B. Oliveira, R.A. Nagem, R.P. de Vries, V.M. Guimarães, Characterization and biotechnological application of recombinant xylanases from *Aspergillus nidulans*, Int. J. Biol. Macromol. 91 (2016) 60–67.
[42] K. Sinma, K. Khucharoenphaisan, V. Kitpreechavanich, S. Tokuyama, Purification and characterization of a thermostable xylanase from *Saccharopolyspora pathumthaniensis* S582 isolated from the gut of a termite, Biosci. Biotechnol. Biochem. 75 (2011) 1957–1963.
[43] S. Kishishita, M. Yoshimi, T. Fujii, L.E. Taylor II, S.R. Decker, K. Ishikawa, H. Inoue, Cellulose-inducible xylanase Xyl10A from *Acremonium cellulolyticus*: purification, cloning and homologous expression, Protein Expr. Purif. 94 (2014) 40–45.
[44] Y. Huang, P.K. Busk, L. Lange, Cellulose and hemicellulose-degrading enzymes in *Fusarium commune* transcriptome and functional characterization of three identified xylanases, Enzym. Microb. Technol. 73 (2015) 9–19.
[45] B. Xu, L. Dai, J. Li, M. Deng, H. Miao, J. Zhou, Y. Mu, Q. Wu, X. Tang, Y. Yang, Molecular and biochemical characterization of a novel xylanase from *Massilia* sp. RBM26 isolated from the feces of *Rhinopithecus bieti*, J. Microbiol. Biotechnol. 26 (2015) 9–19.
[46] Q. Wang, Y. Luo, B. He, L.-S. Jiang, J.-X. Liu, J.-K. Wang, Characterization of a novel xylanase gene from rumen content of Hu sheep, Appl. Biochem. Biotechnol. 177 (2015) 1424–1436.
[47] M. Sudo, M. Sakka, T. Kimura, K. Ratanakhanokchai, K. Sakka, Characterization of *Paenibacillus curdlanolyticus* intracellular xylanase Xyn10B encoded by the xyn10B gene, Biosci. Biotechnol. Biochem. 74 (2010) 2358–2360.
[48] I.T. Hwang, H.K. Lim, H.Y. Song, S.J. Cho, J.-S. Chang, N.-J. Park, Cloning and characterization of a xylanase, KRICT PX1 from the strain *Paenibacillus* sp. HPL-001, Biotechnol. Adv. 28 (2010) 594–601.
[49] T. Fedorova, A. Chulkin, E. Vavilova, I. Maisuradze, A. Trofimov, I. Zorov, V. Khotchenkov, K. Polyakov, S. Benevolensky, O. Koroleva, Purification, biochemical characterization, and structure of recombinant endo-1, 4-β-xylanase XylE, Biochemistry Mosc 77 (2012) 1190–1198.
[50] M. Lafond, A. Tauzin, V. Desseaux, E. Bonnin, E.-H. Ajandouz, T. Giardina, GH10 xylanase D from *Penicillium funiculosum*: biochemical studies and xylooligosaccharide production, Microb. Cell Factories 10 (2011) 20.
[51] F. Zhang, P. Shi, Y. Bai, H. Luo, T. Yuan, H. Huang, P. Yang, L. Miao, B. Yao, An acid and highly thermostable xylanase from *Phialophora* sp. G5, Appl. Biochem. Biotechnol. 89 (2011) 1851–1858.
[52] M.-W. Lai, R.-F. Liou, Two genes encoding GH10 xylanases are essential for the virulence of the oomycete plant pathogen *Phytophthora parasitica*, Curr. Genet. (2018) 1–13.
[53] K. McPhillips, D.M. Waters, C. Parlet, D.J. Walsh, E.K. Arendt, P.G. Murray, Purification and characterisation of a β-1, 4-xylanase from *Remersonia thermophila* CBS 540.69 and its application in bread making, Appl. Biochem. Biotechnol. 172 (2014) 1747–1762.
[54] H. Shi, Y. Zhang, H. Zhong, Y. Huang, X. Li, F. Wang, Cloning, over-expression and characterization of a thermo-tolerant xylanase from *Thermotoga thermarum*, Biotechnol. Lett. 36 (2014) 587–593.
[55] Y. García-Huante, M. Cayetano-Cruz, A. Santiago-Hernández, C. Cano-Ramírez, R. Marsch-Moreno, J.E. Campos, G. Aguilar-Osorio, C.G. Benitez-Cardoza, S. Trejo-Estrada, M.E. Hidalgo-Lara, The thermophilic biomass-degrading fungus *Thielavia terrestris* Co3Bag1 produces a hyperthermophilic and thermostable β-1, 4-xylanase with exo-and endo-activity, Extremophiles 21 (2017) 175–186.
[56] J. de Cassia Pereira, E.C. Giese, M.M. de Souza Moretti, A.C. dos Santos Gomes, O.M. Perrone, M. Boscolo, R. da Silva, E. Gomes, D.A.B. Martins, Effect of metal

ions, chemical agents and organic compounds on lignocellulolytic enzymes activities, in: M. Senturk (Ed.), Enzyme Inhibitors and Activators, InTechOpen, London, 2017.
[57] K. Chiku, J. Uzawa, H. Seki, S. Amachi, T. Fujii, H. SHINOYAMA, Characterization of a novel polyphenol-specific oligoxyloside transfer reaction by a family 11 xylanase from *Bacillus* sp. KT12, Biosci. Biotechnol. Biochem. 72 (2008) 2285–2293.
[58] P.R. Heinen, C. Henn, R.M. Peralta, A. Bracht, R.d.C.G. Simão, J.L. da Conceição Silva, T. Maria de Lourdes, M.K. Kadowaki, Xylanase from *Fusarium heterosporum*: properties and influence of thiol compounds on xylanase activity, Afr. J. Biotechnol. 13 (2014) 1047–1055.
[59] D. Verma, Y. Kawarabayasi, K. Miyazaki, T. Satyanarayana, Cloning, expression and characteristics of a novel alkalistable and thermostable xylanase encoding gene (*Mxyl*) retrieved from compost-soil metagenome, PLoS One 8 (2013) e52459.
[60] V. Kumar, T. Satyanarayana, Biochemical and thermodynamic characteristics of thermo-alkali-stable xylanase from a novel polyextremophilic *Bacillus halodurans* TSEV1, Extremophiles 17 (2013) 797–808.
[61] Y. Bai, J. Wang, Z. Zhang, P. Yang, P. Shi, H. Luo, K. Meng, H. Huang, B. Yao, A new xylanase from thermoacidophilic *Alicyclobacillus* sp. A4 with broad-range pH activity and pH stability, J. Ind. Microbiol. Biotechnol. 37 (2010) 187–194.
[62] H. Shi, Y. Zhang, X. Li, Y. Huang, L. Wang, Y. Wang, H. Ding, F. Wang, A novel highly thermostable xylanase stimulated by Ca^{2+} from *Thermotoga thermarum*: cloning, expression and characterization, Biotechnol. Biofuels 6 (2013) 26.
[63] M. Srinivasan, M.V. Rele, Microbial xylanases for paper industry, Curr. Sci. (1999) 137–142.